Hybrid Line Commutated Converter With Fast Commutation Characteristic Based on IGCT for HVDC Application: Topology, Design Methodology, and Experiments

Chaoqun Xu, Zhanqing Yu, *Member, IEEE*, Biao Zhao, *Senior Member, IEEE*, Zhengyu Chen, Zongze Wang, Chunpin Ren, and Rong Zeng, *Senior Member, IEEE*

***Abstract*—In order to effectively mitigate commutation failure of line commutated converter (LCC), a concept of hybrid converter is proposed. The converter replaces a part of the thyristors by the integrated gate commutated thyristors (IGCT). In this article, the hybrid line commutated converter is further developed and reverse blocking IGCTs (RB-IGCT) are applied in each bridge arm to achieve fast commutation characteristic. RB-IGCT is capable of withstanding bidirectional voltages, and owing to the device control method of self-turn-OFF, has almost zero commutation time and gives play to the advantage of fast commutation, thus earning recovery time for the thyristors. Therefore, the commutation performance of the hybrid converter is enhanced greatly. The topology, control strategy, and the hybrid device characterization analysis with fast commutation are introduced. On the basis, the design methodology of hybrid line commutated converter with fast commutation characteristic (FC-LCC) is presented. Finally, the simulation results based on CIGRE standard system and experimental results of a 30 kV/4.5 kA FC-LCC prototype verify the proposed converter's effectiveness and correctness and the fast commutation characteristic can provide sufficient safety time margin for system. The converter shows promising prospects for high voltage direct current system and has significant value for engineering application.**

***Index Terms*—Commutation failure, design methodology, high voltage direct current (HVdc), hybrid, integrated gate commutated thyristors (IGCT), line commutated converter, thyristor.**

Manuscript received 6 May 2022; revised 12 October 2022; accepted 29 November 2022. Date of publication 1 December 2022; date of current version 14 February 2023. This work was supported in part by Integration projects of National Natural Science Foundation of China-State Grid Joint Fund for Smart Grid under Grant U2166602 and in part by the National Natural Science Foundation of China under Grant 51922062. Recommended for publication by Associate Editor D. Dujic. *(Corresponding authors: Zhanqing Yu; Rong Zeng.)*

Chaoqun Xu, Zhanqing Yu, Biao Zhao, Zongze Wang, Chunpin Ren, and Rong Zeng are with the Department of Electrical Engineering, Tsinghua University, Beijing 100084, China (e-mail: xucq18@mails.tsinghua.edu.cn; yzq@tsinghua.edu.cn; zhao-biao@tsinghua.edu.cn; zzwang132@163.com; 18810903251@163.com; zengrong@tsinghua.edu.cn).

Zhengyu Chen is with the Sichuan Energy Internet Research Institute, Tsinghua University, Beijing 100089, China (e-mail: chenzhen14@tsinghua.org.cn).

Color versions of one or more figures in this article are available at https://doi.org/10.1109/TPEL.2022.3226037.

Digital Object Identifier 10.1109/TPEL.2022.3226037

I. Introduction

HIGH voltage direct current (HVdc) transmission technology has many significant advantages, including long distance, large capacity, low power loss and low construction cost. The advanced HVdc transmission technology has been vigorously developed. The main technical solution is to use line commutated converter (LCC) for ac–dc conversion. It is based on thyristors, the semicontrolled devices that cannot actively turn OFF current [1], [2]. Therefore, the ac grid voltage is required for the natural current commutation. However, when the ac grid voltage is disturbed or the converter system has an internal fault, it is easy to cause commutation failure (CF) of the inverter at the receiving end, resulting in interruption of dc power transmission and overvoltage at the sending end.

Recently, a lot of research about mitigating CF of LCC-HVdc system has been conducted [3], [4], [5], [6], [7], [8]. The method of mitigating CF can be typically divided into two categories, the advanced converter topology and the improved control strategy. However, these methods are still difficult to significantly reduce the risk of CF under all operating conditions. They are also difficult to apply in engineering projects due to modification costs.

Due to the inherent recovery characteristics of thyristors, it is difficult to significantly mitigate CF through the existing conventional methods. As we know, integrated gate commutated thyristor (IGCT) has made considerable progress in manufacturing process and operating losses. This is a kind of device originated from thyristor but with controllable turn-OFF capability [9], [10]. However, the commercial IGCT only has the ability to block the forward voltage, which is the asymmetrical IGCT. The reverse blocking IGCT (RB-IGCT) is further developed, with the ability to block voltages in both forward and reverse directions and to actively turn OFF the forward current [11]. The current capacity and reliability of IGCTs are similar to those of thyristors, but the ON-state voltage is much lower than that of the other controllable turn-OFF devices, including insulated gate bipolar transistor (IGBT) [12], [13]. At the same time, compared with IGBT, IGCT has a more mature manufacturing process and lower manufacturing cost [14]. At the same time, reverse blocking IGBTs (RB-IGBTs) are restricted by their chip

structure. They require edge blocking technology to occupy as little chip area as possible, which makes it difficult to achieve high bidirectional voltage withstanding ability. At present, the performance of various parameters is not good for RB-IGBT [15]. On contrast, the IGCT is a whole wafer structure, which can achieve higher blocking voltages through edge grinding and passivation, which has advantages on parameter performance and manufacturing process. Therefore, as a reverse blocking turn-OFF device for high-voltage and large-capacity, IGCT is the preferred device. And RB-IGCT can be equivalent replaced by asymmetrical IGCT in series with diode.

The concept of a hybrid LCC is proposed by Xu et al. [16]. The hybrid converter replaces a part of the thyristors by the IGCTs. It utilized the active turn-OFF principle of IGCT to achieve the forced commutation characteristics. However, it is limited by the maximum repetitive turn-OFF current capability of the IGCT. By the active turn-OFF principle, the dynamic voltage equilibrium is especially difficult to achieve among hybrid IGCTs and thyristors. The topology, the analysis, the commutation principle and the design methodology of the converter has not been deeply conducted. Moreover, the hybrid device characterization of IGCT and thyristor in HVdc applications is not reported in existing literatures. In fact, there is little research on dc equipment based on hybrid devices. The IGCT/IGBT hybrid dc circuit breaker was reported [17], but it was only a single-breaking working condition, which is significantly different from the commutation condition of high voltage converters. The types of semicontrolled and fully-controlled devices are different. The multifield coupling stress is not clear. Therefore, there is a lack of theoretical and technical research on the LCC-HVdc based on hybrid devices of IGCT and thyristor. The interaction mechanism between the internal carrier behavior of power devices and the external snubber circuits is unclear, and the interaction between these two types of devices is unclear. The static and dynamic voltage equalization, and stress analysis method are lack of theoretical and practical basis. Therefore, the article focuses on the hybrid topology, hybrid control strategy, and the hybrid device characterization analysis with interaction of IGCT and thyristor for fast commutation.

In this article, its beneficial advantage is that this hybrid topology can use the characteristics of RB-IGCT to realize a new auxiliary commutation principle, which is going to be proposed. On the basis of the abovementioned description, the hybrid converter with fast commutation characteristic (FC-LCC) and its topology, design methodology, and experiments are going to be revealed in this article.

Therefore, to address the aforementioned gap, the rest of this article is organized as follows. Section II presents the proposed FC-LCC topology with fast commutation characteristic and the novel control strategy. Section III demonstrates the corresponding hybrid device characterization analysis of IGCT and thyristor for fast commutation, and on the basis, Section IV presents the design methodology of FC-LCC. On the basis, the simulation validation and experimental verification are carried out, respectively, in Section V and VI. The comprehensive performance analysis of proposed FC-LCC is conducted. A 30 kV/4.5 kA FC-LCC prototype is built to verify the effectiveness and correctness. Finally, Section VII concludes this article.

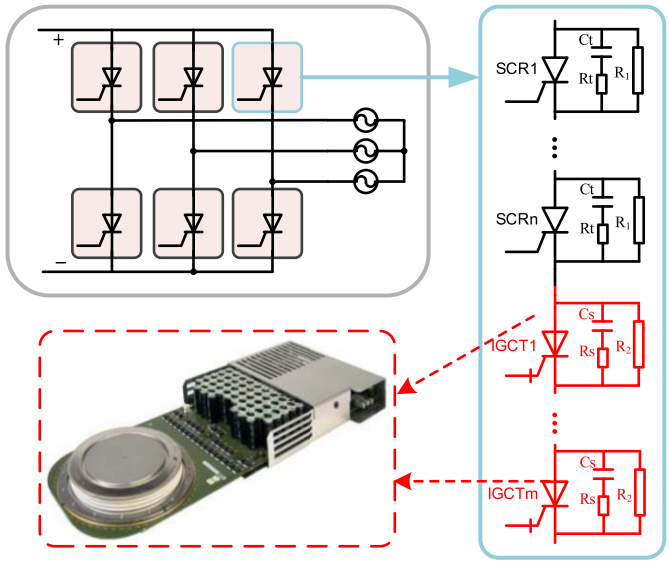

Fig. 1. Diagram of the proposed FC-LCC topology with fast commutation characteristic.

II. Proposed FC-LCC Topology and Fast Commutation Control Strategy

A. FC-LCC Topology With Fast Commutation Characteristic

The proposed FC-LCC topology is presented in Fig. 1. Each arm is composed of original thyristors and a certain percentage of IGCTs. They are series-connected so it can be considered that in each arm, a certain percentage of thyristors are replaced by IGCTs. Therefore, the proposed converter can be applied in the existing HVdc converter stations without complex renovation. It is especially appropriate for simply replace thyristor with IGCT one to one.

Compared with IGBT, IGCT has the following advantages in the proposed FC-LCC, including long-term reliable short-circuit failure mode, and higher voltage rating, as well as the operating loss. The recovery speed of IGCT is faster than that of thyristor, and has controllable withstanding voltage capability. With the help of gate drive unit of IGCT, IGCT has almost zero commutation time, which gives an opportunity to create fast commutation characteristic.

Parallel to thyristors and IGCTs, the snubber circuits including snubber resistor and capacitor are designed. Because the commutation time and voltage establishment speed of IGCT and thyristor are different, the parameters of snubber circuit should be regulated to realize fast commutation characteristic. The design methodology of the snubber circuits is introduced in Section IV.

B. Control Strategy for Fast Commutation of FC-LCC

In the proposed FC-LCC, RB-IGCT can be replaced by asymmetrical IGCT in series with diode to achieve bidirectional blocking voltage capability. Therefore, when studying the

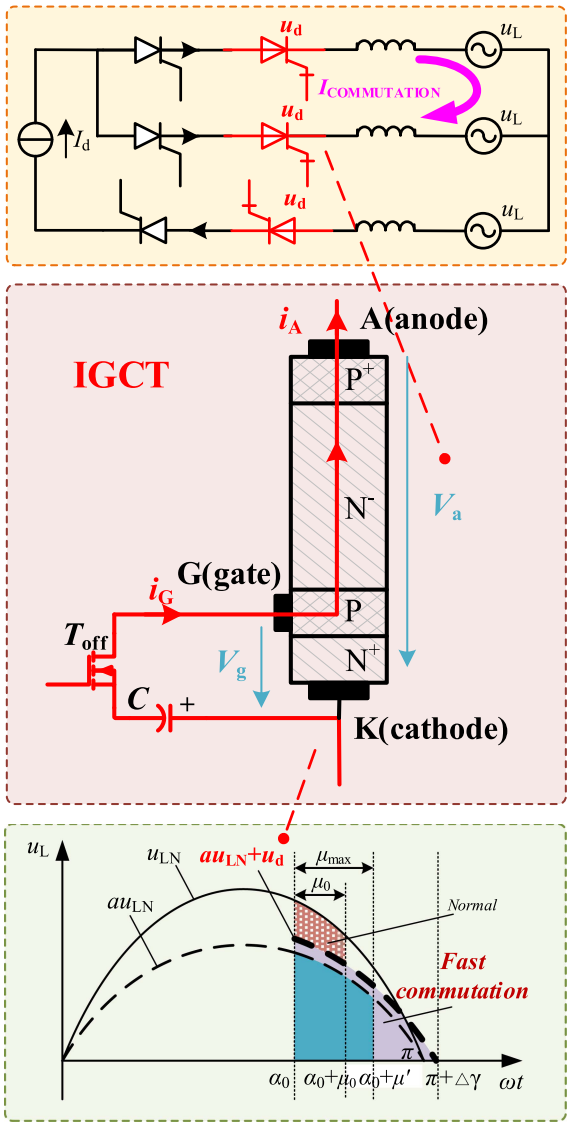

Fig. 2. Control strategy and new commutation principle for fast commutation.

commutation process, as presented in Fig. 2, take asymmetrical IGCT with diode structure as an example to explain the control strategy and commutation principle for fast commutation. The operation principle of RB-IGCT should be easier to implement than asymmetrical IGCT with diode as it is an independent device. During commutation process in FC-LCC, the control strategy of IGCT device is described as follows.

When the current of asymmetric IGCT i_A crosses zero and the IGCT is applied with negative voltage by the external circuit, since asymmetrical IGCT is a unidirectional voltage withstanding device, the negative voltage will be applied to the series-connected diode. After the line current crosses zero, the IGCT will trigger a self-turn-OFF signal. The optimized method is that when the current i_A crosses zero, the series-connected diode will first start recovery process, and the recovery time of series-connected diode is very short, only a few microseconds. At this time period, due to the recovery process of the diode, a reverse current i_A flows through the IGCT, as presented in Fig. 2. Therefore, a small negative voltage V_a will be generated at IGCT. The value of this negative voltage V_a is determined by the voltage drop characteristic of the IGCT's J_1 and J_2 junction. The gate drive unit of IGCT can detect this change, so that it can give IGCT a self-turn-OFF signal. The self-turn-OFF signal will control the MOSFET T_{OFF} of the gate drive unit. The capacitor C in the gate drive unit will keep IGCT in the blocked state. Therefore, the IGCT can be regarded as a controllable thyristor with a commutation time near zero. The commutation time depends on the characteristics of the IGCT itself, the di/dt of the external circuit and the gate drive unit detection speed.

Because the commutation time of IGCT can be very low, the withstanding voltage of IGCT can give an increase of the commutation ac voltage, which facilitates the commutation process, give play to the advantage of fast commutation. The principle is illustrated, as presented in Fig. 2. During normal operation, the commutation process is driven by line voltage u_{LN}. The corresponding commutation angle is μ_0. When the ac power grid disturbs and has a voltage drop to au_{LN}, the commutation will be slow and the maximum commutation angle is μ_{max}. The commutation failure is about to occur while the IGCT can compensate this voltage drop and raise the commutation voltage to $au_{LN}+u_d$. With the high commutation voltage, the commutation process is shortened. Therefore, the commutation performance of the FC-LCC is enhanced greatly, thus mitigating commutation failure.

III. Hybrid Device Characterization Analysis With Fast Commutation Characteristic

The proposed FC-LCC topology has hybrid bridge arms with fast commutation characteristic, which are composed of IGCTs and thyristors.

A. Thyristor Device Commutation Characterization Analysis

During the commutation, Fig. 3(a) shows the current and voltage waveforms of the thyristor. i_A is the anode current of the thyristor, and v_{AK} represents the anode voltage of the thyristor. In the commutation process, the thyristor structure changes and behaves as the following illustrations.

1) t_0-t_1, the thyristor is fully turned-ON at the beginning, as presented in Fig. 3(b). When the applied voltage changes from forward to reverse, due to the external circuit inductance, the current through the inductor and the thyristor in a short period of time t_0-t_1 can be regarded as decay at a constant rate, and the di/dt at this time period is often very large, so the time interval between t_0-t_1 is very small compared to the carrier lifetime, so when the current crosses zero, there is still a high carrier concentration in the thyristor, which is the carrier storage area.
2) t_1-t_2, at this time period, the current through the thyristor has reversed, the excess carriers are swept away in the base, and the sweeping of the carriers leads to a substantial decrease of the carrier concentration in the body.
3) t_2-t_3, at this time period, the carriers in the J_3 junction of the thyristor are swept away, and the J_3 junction begins to be able to withstand voltage. There are two reasons, firstly

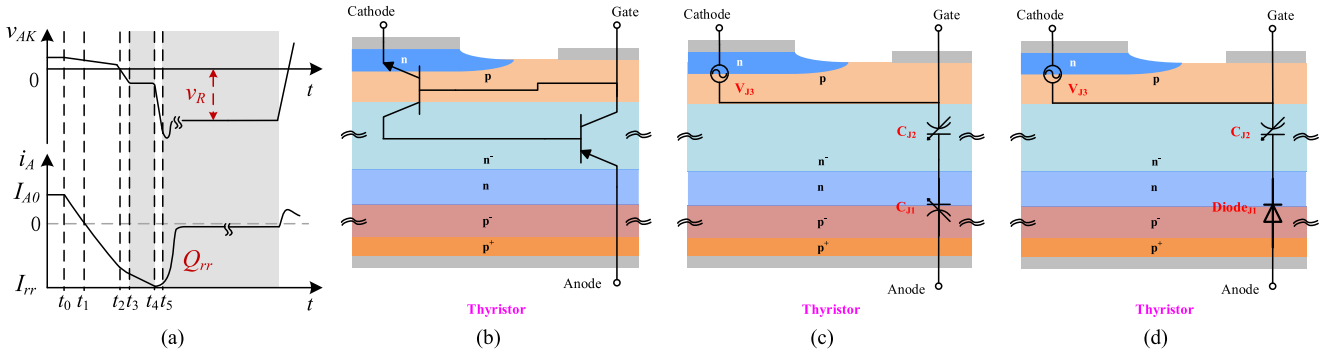

Fig. 3. Commutation characterization analysis of thyristor. (a) Current and voltage waveforms of the thyristor. (b) Thyristor structure characterization during conduction. (c) Thyristor structure characterization during t_3-t_4. (d) Thyristor structure characterization after t_5.

the p-base region is more heavily doped than the n-base region, and secondly the carrier concentration of the p^+ emitter is higher than that of the n^+ emitter.

4) t_3-t_4, at this time period, the anode voltage of the thyristor reaches the avalanche breakdown voltage of the J_3 junction, and then the J_3 junction will behave like a voltage source, and this voltage is often 17–20 V in amplitude, which is determined by the doping concentration of J_3 junction. The J_3 junction at this stage can be regarded as a critical breakdown state, with clamping voltage characteristics. It behaves as Fig. 3(c).
5) t_4-t_5, at this time period, the excess carrier concentration of the J_1 junction drops to zero, and the J_1 junction begins to withstand the reverse voltage. At this stage, the J_1 junction exhibits diode characteristics.
6) After t_5, the reverse current begins to decrease. When $|V_{AK}|$ is larger than the bus voltage of the device, it causes the di/dt value reverse, as the power load is usually inductive in converters.
7) When the reverse current decays, the J_2 junction of the thyristor gradually sweeps away the carriers, and the depletion region of the J_2 junction is gradually established. With the establishment of the depletion layer, the thyristor gradually gains the ability to withstand the forward voltage. During the process, with the gradual sweeping of carriers, the J_2 junction can be equivalent to a variable capacitor. The capacitor has a constant breakdown voltage value when it is subjected to a forward voltage. When it is subjected to a reverse voltage, its capacitance value gradually decreases with the process of the sweeping, and finally behaves as a diode characteristic, which is illustrated in Fig. 3(d).

Therefore, based on the abovementioned analysis, the recovery time can be estimated. It is assumed that the carrier concentration of the entire thyristor body is constant. The decrease of carrier concentration after turn-OFF can be calculated by the continuity equation. The solution is

$$n(t) = n_1 e^{-\frac{t}{\tau}} + n_0 \tag{1}$$

where n_1 is the initial value of the carrier concentration when the bridge arm current of FC-LCC drops to zero.

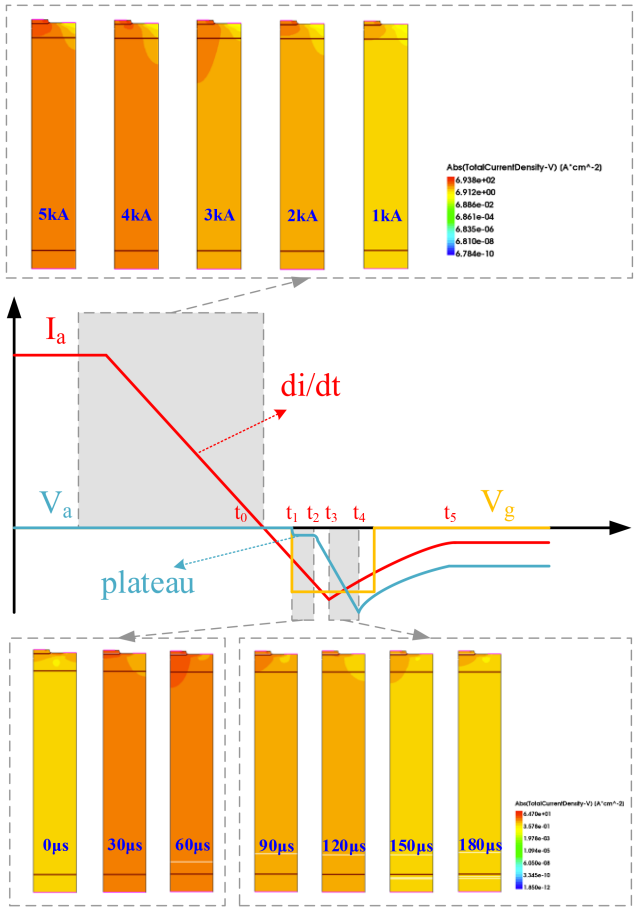

Fig. 4. Commutation characterization of IGCT in FC-LCC.

The typical carrier concentration in the thyristor during conduction is 10^{16}-10^{17} cm^{-3}, which is 3–4 orders higher than the doping concentration in the base region, so its commutation time is about ten carrier life cycles, which is about hundreds of microseconds.

B. IGCT Device Commutation Characterization Analysis

Typically, the fast commutation process of IGCT device in FC-LCC is analyzed as follows. It is presented in Fig. 4.

At t_0, the anode current i_a crosses zero, and the IGCT device starts its recovery phase.

At t_1, the J_3 junction first begins to withstand voltage. At this time, the gate drive unit is not connected into the circuit. The reverse voltage is determined by the avalanche breakdown voltage of the J_3 junction. At the same time, the anode-cathode voltage V_a has a short plateau. At this time, the reverse voltage V_a is equal to the gate voltage V_g. The depletion layer of the J_1 junction has not been established.

At t_2, the J_1 junction begins to establish a depletion layer. After the holes of diffusing current enter the space charge region on both sides of the J_1 junction, they are quickly pulled to the anode by the built-in voltage, and the voltage is quickly established. The excess carriers at the J_3 junction decay to zero faster than the J_1 junction.

At t_3, the reverse current reaches its peak value and begins to decrease. This is because the carrier concentration of remaining excess carriers begins to decrease, resulting in a decrease in carriers diffused to the edge of the depletion layer. At this time, the anode reverse voltage V_a is equal to the reverse voltage applied by the external circuit. As the current begins to decrease, the voltage drop generated on the inductor will continue to increase the anode voltage, causing an overshoot voltage across the device. Importantly, it cannot exceed the reverse breakdown voltage.

At t_4, the voltage of J_3 junction returns to zero, and finally the reverse voltage is withstood by the J_1 junction.

On the basis, a simulation with finite element analysis based on Sentaurus/Technology Computer Aided Design is performed to observe the relationship between the change of internal carrier concentration of IGCT and the external current and voltage stress, as shown in Fig. 4. The carrier concentration of GCT chip is presented for the fast commutation process.

Therefore, the IGCT device commutation characterization enjoys a fast carrier extraction process, thus, the fast commutation characteristic is realized.

IV. Interaction and Design Methodology of FC-LCC for Fast Commutation

A. Interaction of Voltage and Current Stress of Hybrid IGCT and Thyristor in Series Connection

On the basis of hybrid device characterization analysis in Section III, for fast commutation process, the voltage and current stress coordination of hybrid IGCT and thyristor can be disassembled and analyzed as follows, the simplified topology structure of FC-LCC including the snubber circuits is presented in Fig. 5 to give a clear description.

1) t_0-t_1, under the forced commutation of the ac voltage of the external circuit, the current through the thyristor and IGCT decays rapidly, and the current rate di/dt is determined by the inductance value of the external circuit and the ac voltage value

$$U_s = L_1 \cdot {}^{di}/_{dt} \tag{2}$$

where U_s is the external ac voltage, L_1 is the inductance.

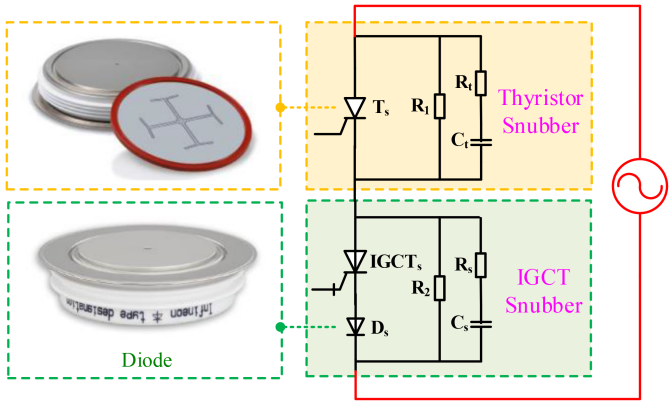

Fig. 5. Simplified topology of FC-LCC including snubber circuit.

2) t_1-t_2, the carriers of J_3 junction of the thyristor are first swept away, and the voltage across the thyristor reaches the avalanche breakdown voltage of the J_3 junction. Therefore, the J_3 junction behaves like a voltage source, and the voltage is clamped at about 20 V. That is, the J_3 junction is in a critical breakdown state. Due to the low carrier concentration of J_3 junction, the sweep is very fast, and the process at this stage is less than 1 μs.
3) t_1-t_3, the diode in series with asymmetrical IGCT starts its recovery process as the current drops to zero. During the recovery process, as explained previously, the asymmetrical IGCT gate drive unit starts detection and will give the IGCT a self-turn-OFF signal. At t_3 moment, the diode completes recovery, after which it can withstand the reverse voltage. Since the series-connected diode is a fast recovery diode, its recovery time is about 2–5 μs. If the series-connected diode is a standard diode, it should be 20–50 μs

$$U_s'(t_3) = V_{Cs} \tag{3}$$

where V_{Cs} is the voltage of the snubber capacitor C_s.
4) t_2-t_4, then, the carriers of the J_1 junction of the thyristor will be swept out, and the J_1 junction can establish a depletion layer when it is subjected to a reverse voltage, which shows the characteristics of diode. At t_4, the J_1 junction of the thyristor is restored and can withstand reverse voltage thereafter.
5) t_4-t_5, the ac voltage of the external circuit is dynamically distributed between the snubber capacitor of the IGCT, the equivalent capacitor of the thyristor J_2, and the snubber capacitor of the thyristor. At the same time, it is affected by the inductance and a certain degree of oscillation is induced. During this period, the relationship of voltages and charges can be listed as

$$\begin{cases} U_s'(t_4) = V_{Cs}(t_4) \\ U_s'(t_5) = V_{Cs}(t_5) + V_{Ct}(t_5) \\ i = C_s \frac{d(V_{Cs}(t_5) - V_{Cs}(t_4))}{t_5 - t_4} = (C_{J2} + C_t) \frac{d(V_{Ct}(t_5) - 0)}{t_5 - t_4} \\ \Delta Q = |C_s(V_{Cs}(t_5) - V_{Cs}(t_4))| \\ \quad = |(C_{J2} + C_t)(V_{Ct}(t_5) - 0)| \end{cases} \tag{4}$$

where V_{Ct} is the voltage of the snubber capacitor C_t, C_{J2} is the equivalent capacitance of J_2 junction.

6) From t_5-t_6, at t_6, the thyristor J_2 junction completes recovery. After t_6, the thyristor regains the ability to withstand the forward voltage. t_1–t_6, called the commutation time of the thyristor, is often hundreds of microseconds, but it is also affected by the recovery characteristics of the thyristor itself, the external voltage, di/dt, and recovery current.
7) t_5–t_7, the ac voltage of the external circuit varies from negative to positive. t_7 is the moment that the ac voltage of the external circuit varies from negative to positive. If the thyristor has recovered, the thyristor can withstand the positive voltage; if the thyristor has not completed the recovery, the IGCT can withstand the positive voltage, which is denoted as

$$\begin{cases} U_s'(t_7) = V_{Cs}(t_7) + V_{Ct}(t_7) \\ C_s V_{Cs}(t_7) = -C_t V_{Ct}(t_7). \end{cases} \tag{5}$$

To sum up, the voltage stress during the fast commutation is presented as above. The current stress during the fast commutation has no difference with the conventional LCC converter.

B. Design Methodology of Proposed FC-LCC

Based on the abovementioned analysis, for fast commutation process, we can get the parameters of snubber resistor and capacitor of thyristor and IGCT in Fig. 5. In order to ensure that when the ac voltage is positive, the IGCT tolerates the positive voltage, not the thyristor, thus earning more recovery time for the thyristor. These equations of (3), (4), and (5) can be expressed and presented as

$$\begin{cases} U_s'(t_6) = V_{Cs}(t_6) + V_{Ct}(t_6) \\ C_s \frac{d(V_{Cs}(t_6) - V_{Cs}(t_4))}{t_6 - t_4} = (C_{J2} + C_t) \frac{d(V_{Ct}(t_6) - 0)}{t_6 - t_4} \\ |C_s (V_{Cs}(t_6) - V_{Cs}(t_4))| = |(C_{J2} + C_t)(V_{Ct}(t_6) - 0)| \\ \frac{U_s'(t_6)}{R_s + R_t}(t_6 - t_4) = (C_{J2} + C_t)(U_s'(t_4) - 0) \\ C_s \frac{d(V_{Cs}(t_7) - V_{Cs}(t_6))}{t_7 - t_6} = C_t \frac{d(V_{Ct}(t_7) - V_{Ct}(t_6))}{t_7 - t_6} \\ \frac{U_s'(t_7)}{R_s + R_t}(t_7 - t_6) = C_t (V_{Ct}(t_7) - V_{Ct}(t_6)) \end{cases} \tag{6}$$

where the equivalent capacitance C_{J2} of the J_2 junction of the thyristor is time-varying, which means

$$\begin{aligned} &U_s'(t_7) = V_{Cs}(t_7) + V_{Ct}(t_7) > 0 \\ &V_{Cs}(t_7) > 0 \\ &V_{Ct}(t_7) < 0. \end{aligned} \tag{7}$$

From the abovementioned relationships (6) and (7), it can be obtained that the value of the snubber capacitor C_s matched with IGCT as presented in

$$C_s = \frac{U_s'(t_7)(t_7 - t_6)}{(R_s + R_t)} \cdot \frac{1}{U_s'(t_7) - \left(2\frac{(C_{J2} + C_t)U_s'(t_4)(R_s + R_t)}{(t_6 - t_4)} - U_s'(t_6)\right)}. \tag{8}$$

TABLE I
DESIGN OF SNUBBER CIRCUIT IN CONVERTER FOR FAST COMMUTATION

Device	ITEM	Value
Thyristor	Snubber resistor	25 Ω
	Snubber capacitor	1.1 μF
	Static equivalent resistor	800 kΩ
IGCT	Snubber resistor	1.2 Ω
	Snubber capacitor	1 μF
	Static equivalent resistor	300 kΩ

TABLE II
TYPICAL PARAMETERS OF THYRISTOR AND IGCT IN CONVERTER

Parameters	Thyristor	IGCT
Off-state repetitive peak voltage	8500 V	4500 V
Dc continuous current	5500 A	3000 A
Off-state repetitive peak current	⩽25 mA	⩽50 mA
On-state Dc voltage	1.8 V	2.6 V
On-state non repetitive surge current	58 kA	35 kA
Critical rise rate of on-state current	500 A/μs	5000 A/μs
Critical rise rate of off-state voltage	4000 V/μs	1000 V/μs

It should be mentioned that the value of C_s is closely related to the equivalent capacitance of the thyristor and the commutation time.

The value of the snubber resistor R_s matched with the IGCT can be selected according to the anode current when the IGCT is turned ON

$$\frac{V_{Cs}(t_7)}{I_{\text{main}}} > R_s > \frac{V_{Cs}(t_7)}{I_{\max}} \tag{9}$$

where I_{main} is the rated anode current of IGCT and $I_{\max}$ is the maximum anode current of IGCT in converter.

Finally, on the basis of the design methodology, the design example of the snubber circuit of the proposed FC-LCC is presented in Table I. The snubber resistance of thyristor is 25 Ω. The snubber capacitance of thyristor is 1.1 μF. The static resistance is 800 kΩ. Respectively, the snubber resistance of IGCT is 1.2 Ω. The snubber capacitance of IGCT is 1 μF. The static equivalent resistance is 300 kΩ according to the rated ac voltage of IGCT. The values of the snubber circuit listed in Table I are extracted from the typical commercial devices of IGCT and thyristor. The parameters of thyristor and IGCT are from their datasheets in [18] and [19], and listed in Table II.

Based on the parameter design, a 30 kV level prototype of the proposed FC-LCC is built in Section VI for experimental validation.

V. SIMULATION STUDY

A. Simulation Study System

In order to verify the effectiveness of fast commutation characteristic for the proposed FC-LCC, a study system is built in PSCAD/EMTdc based on the CIGRE benchmark model.

The parameters of the study system and the converter are presented in Table III. The capacity of the IGCT device in one

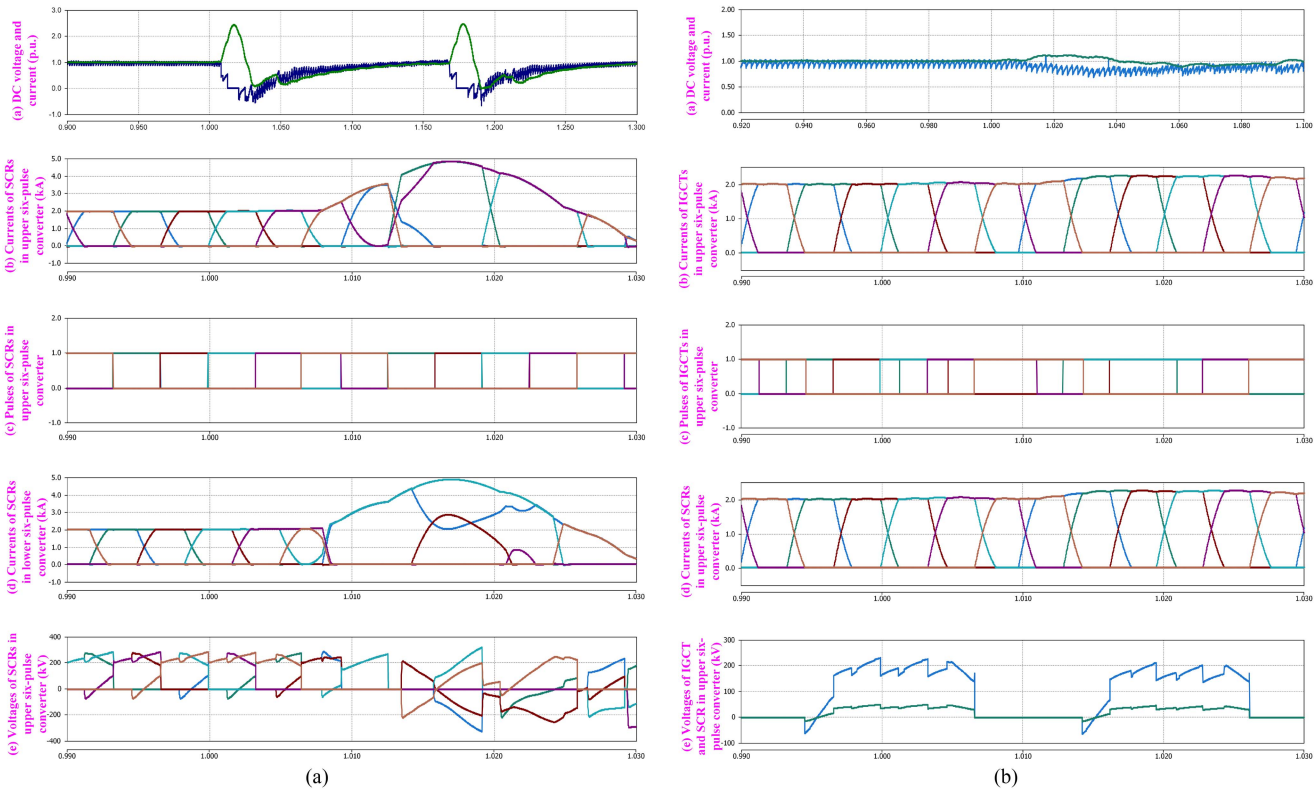

Fig. 6. Simulation waveforms. (a) Conventional LCC. (b) Proposed FC-LCC with fast commutation.

TABLE III
STUDY SYSTEM PARAMETERS

Items	Rectifier	Inverter
Ac system voltage (kV)	345	230
SCR	2.5	2.5
Leakage inductance	18%	18%
Dc voltage (kV)	500	500
Dc current (kA)	2.0	2.0
Dc resistor (Ω)	5	
Dc inductance (H)	1.1936	

bridge arm can be varied between 0% to 100%. The typical percentage of IGCT should be 30%, 50%, and 100%, thus, the corresponding percentage of thyristor is 70%, 50%, and 0%.

B. Investigation on Fast Commutation Characteristic and CF Mitigation Capability

The simulation waveforms are presented in Fig. 6(a) and (b). The comparison between the FC-LCC and the conventional LCC with $t_q = 400$ μs is shown. To give a clear illustration of the fast commutation process, an ac grid grounding inductive fault occurs at $t = 1.0$ s and lasts for 0.3 s.

As shown in Fig. 6(a) of conventional LCC, when t = 1.0 s, after the ac fault occurs and then the CF occurs, the dc current rises from 1 to 2.5 p.u., the dc voltage falls to 0 p.u., respectively, as shown in Fig. 6(a)-(a). The currents of thyristors in upper six-pulse converter and lower six-pulse converter rise to 5.0 kA at most, as shown in Fig. 6(a) and (b) and Fig. 6(a)–(d). The pulses of thyristors in upper six-pulse converter are presented in Fig. 6(a)–(c). Because the fault occurs at the ac grid end, the conventional LCC cannot ride through the fault and the CF occurs consequently. During the commutation failure, the thyristors in upper six-pulse converter withstand higher negative voltage, as presented in Fig. 6(a)–(e).

In the proposed FC-LCC with fast commutation characteristics, as shown in Fig. 6(b), under the same ac fault, owing to the IGCT and control strategy proposed in the manuscript for fast commutation, the commutation process still completes, The dc current rises from 1 to 1.1 p.u., and dc voltage falls to 0.75 p.u, as shown in Fig. 6(b)-(a), because of the dc system oscillation caused by the ac fault. The currents of thyristors and IGCTs in upper six-pulse converter remain nearly 2.0 kA and rise to 2.2 kA at most, as shown in Fig. 6(b)-(b) and Fig. 6(b)–(d). The pulses of IGCTs in upper six-pulse converter during commutation failure are presented in Fig. 6(b) and (c). After the fast commutation, the IGCTs and thyristors in one bridge arm of the upper six-pulse converter share the voltage establishment, as presented in Fig. 6(b)–(e). The voltage distribution is determined by the configuration of IGCT. Therefore, as shown in Fig. 6(b), the proposed FC-LCC can ride through the fault and CF does not occur. It can be concluded that from the simulation study, the withstanding voltages of IGCTs give an increase of the commutation voltage, which facilitates the

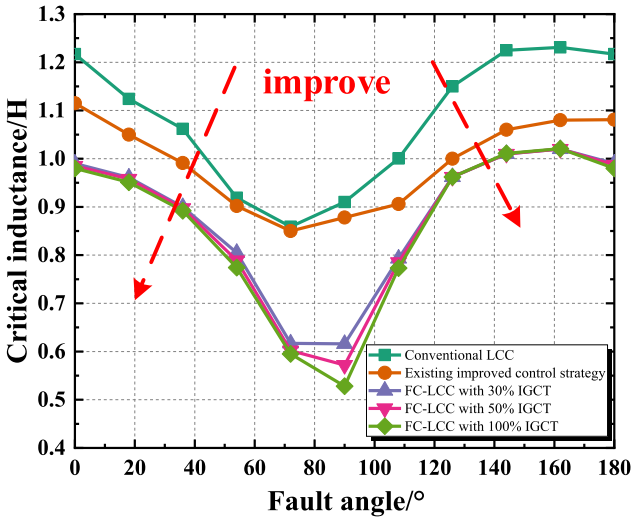

Fig. 7. Investigation of commutation failure mitigation capability.

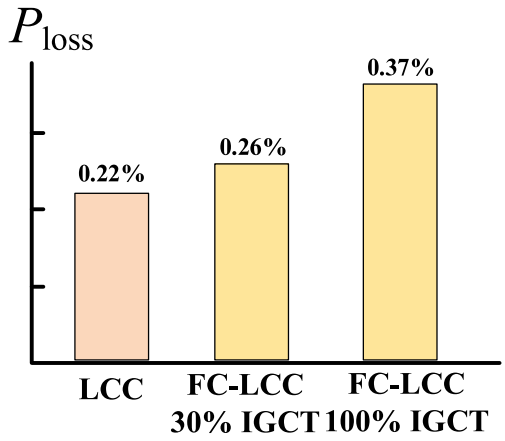

Fig. 8. Operating power losses analysis between 30% IGCT of FC-LCC, 100% IGCT of FC-LCC, and the conventional LCC.

commutation process. With the high commutation voltage, the commutation process is shortened.

In the abovementioned simulation cases, in this article, to quantify the CF mitigation capability, the critical inductance at the receiving ac grid is applied in the analysis. Phase to ground inductive faults are used at the inverter bus to study the performance of FC-LCC and IGCT on CF mitigation. The conventional LCC based on thyristors, LCC with improved control strategy, and the proposed FC-LCC with 30% IGCT, 50% IGCT, and 100% IGCT are comprehensively compared. The converter parameters are all the same. The phased to ground faults are applied at different times with a 18° step. The quantitative CF mitigation capability results are presented in Fig. 7.

It can be seen that the results of conventional LCC are 0.86–1.23 H and that with existing improved control strategy are 0.85–1.12 H, respectively. The proposed FC-LCC with 30% IGCT can decrease the critical inductance to 0.62 H. Generally, 50% IGCT and 100% IGCT can decrease the critical inductance to 0.57 H and 0.53 H, respectively. At different fault angles, the three curves of FC-LCC with 30% IGCT, 50% IGCT, and 100% IGCT almost coincide. In the analysis, the lower the critical grounding inductance, the stronger the capability to mitigate commutation failure. Therefore, the proposed FC-LCC can improve the CF mitigation capability of the HVdc system.

On the basis of the demonstrated fast commutation principle, the IGCTs give an increase of the commutation voltage, which facilitates the commutation process. The commutation voltage also gains more recovery time for thyristors. We consider the most severe working conditions, and the ac system gives the thyristors the shortest recovery time, which is zero. It requires the IGCTs earn more than 400 μs for the thyristors. After the ac voltage crosses zero from negative to positive, the IGCTs should generate the sufficient commutation voltage for more than 400 μs. Therefore, the percentage of IGCT should be higher than 30%, considering a certain ac voltage change rate.

In ultra-HVdc engineering, thousands of thyristors are used in a station. The method to replace certain percentage of thyristors with IGCTs is more efficient and economical. Reconstruction of converter stations is also more feasible.

A comprehensive analysis of the power loss comparison between 30% IGCT of FC-LCC, 100% IGCT of FC-LCC, and the conventional LCC is conducted. The ON-state voltages of IGCT and thyristor are estimated to be 2.6 V and 1.8 V, respectively. IGCT inherits the characteristics of thyristor, including the low ON-state voltage. In FC-LCC, the IGCT operates self-turn-OFF principle when commutation failure occurs, the turn-OFF loss of IGCT can be ignored. The recovery losses of IGCTs and thyristors are extracted from the datasheets given by the manufacturers [18], [19]. A calculation model is established on the basis of commutation characteristics of IGCTs and thyristors. The comparison of power losses between 30% IGCT of FC-LCC, 100% IGCT of FC-LCC, and the conventional LCC is presented in Fig. 8. The power loss of the conventional LCC is 0.22%. The power loss of FC-LCC with 30% IGCT is 0.26%, and for comparison, that of the FC-LCC with 100% IGCT is 0.37%.

A comprehensive analysis of the economic cost comparison of FC-LCC between 30% IGCT and 100% IGCT is also conducted. For the FC-LCC with 30% IGCT, 30% of the thyristors are replaced by IGCTs. The additional economic cost when reconstruction is relatively low. For the FC-LCC with 100% IGCT, it can be considered that the components of the original LCC converter are removed. The manufacturing costs of thyristor and IGCT are given by the manufacturers. On the basis of device cost, the economic cost comparison of conventional LCC and proposed FC-LCC is presented in Table IV. The economic costs of a FC-LCC converter valve with 30% IGCT and 100% IGCT increase to 1.2 times and 1.3 times of that of conventional LCC.

A comprehensive analysis of the structural volume is then conducted. Because the IGCT integrates the gate drive unit and GCT chip together, the volume of IGCT itself is a little larger than that of thyristor. We can conclude that the converter valve composed of IGCT will be larger than the converter valve composed of thyristor.

TABLE IV
ECONOMIC COST ANALYSIS

Converter	Conventional LCC	FC-LCC with 30% IGCT	FC-LCC with 100% IGCT
Type	same device connection	hybrid device connection	same device connection
Number of power devices	N thyristors	0.7N thyristors and 0.3N IGCTs	N IGCTs
Economic cost of a converter valve	1.0 p.u.	1.2 p.u.	1.3 p.u.
Structure	simple	simple	simple
Volume	small	small	large

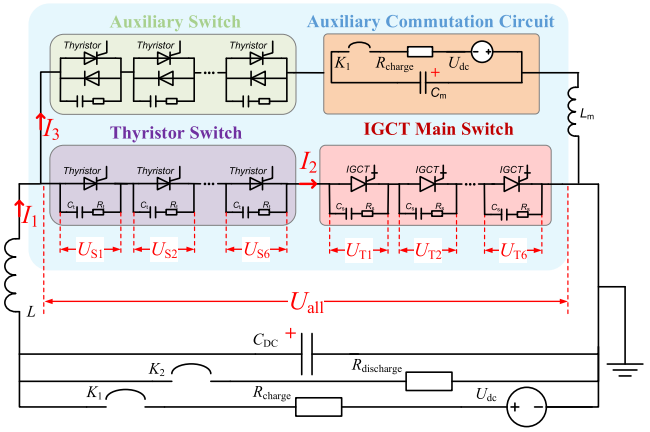

Fig. 9. Diagram of experimental circuit, including the two LC oscillation circuits to modify the operating conditions and perform the commutation process of the proposed FC-LCC in HVdc application.

It is thus claimed from the comprehensive analysis that the proposed FC-LCC with 30% IGCT has advantages in operating power losses and economic cost, compared with 100% IGCT.

VI. EXPERIMENTAL VALIDATION

A. Development of FC-LCC Prototype and Test Scheme for Fast Commutation

In the article, a 30 kV/4.5 kA prototype of the proposed FC-LCC based on IGCT is built for experimental validation of fast commutation characteristic. Six IGCTs and diodes are applied and in series-connected with snubber circuits to form the equivalent RB-IGCTs. The asymmetrical IGCT-Plus device is used in the prototype, whose parameters are in [18]. Six thyristors are series-connected and applied with snubber circuits as the thyristor switch. Therefore, the IGCT main switch and the thyristor switch are composed as FC-LCC prototype. A 60 kV thyristor and antiparallel diode module is built to behave as an auxiliary switch in the experiments.

The experimental circuit is presented in Fig. 9. Before experiments, Capacitor C_{dc} is precharged to a certain value by the charging circuit, which is composed of U_{dc}, R_{charge}, and K_1. C_{dc} and L are operated to oscillate to create a flowing alternating current. Capacitor C_m is reverse charged to generate a commutating voltage source, pushing the current from one bridge arm to the adjacent bridge arm. The polarity is shown in the Fig. 9. Inductor L_m is chosen to adjust the di/dt value in the experiments. $R_{discharge}$ and K_2 are the discharging circuit for the capacitors in the experiments. This two LC oscillation circuits are built to modify the operating conditions and perform the commutation process of the proposed FC-LCC in HVdc application.

B. Experimental Results

The experimental prototype is shown in Fig. 10(a). The experimental platform is shown in Fig. 10(b), including the auxiliary switch, thyristor switch, IGCT switch, auxiliary commutation circuit, and testing equipment. The prototype applies the proposed topology and control strategy for fast commutation as mentioned in the abovementioned sections. The experimental waveforms are in Fig. 10(c) and (d).

In the experiments, the 30 kV/4.5 kA FC-LCC prototype applies the proposed topology and control strategy for fast commutation characteristics to mitigate commutation failure. We can see that IGCT in series connection with diode is faster in the commutation process than thyristor. As shown in Fig. 10(c), before experiment, C_{dc} and C_m are precharged. Then, the IGCT main switch and thyristor switch are conducted on, and C_{dc} and L_{dc} generate a current of 4.5 kA before commutation, which is denoted as I_1. The current that flows through IGCT main switch and thyristor switch is denoted as I_2. Then, the auxiliary thyristor switch turns ON, the voltage source of capacitor C_m works, commutating current from I_2 to I_3. The current that flows through auxiliary switch is denoted as I_3. After the current I_2 crosses zero, the ac voltage is negative, and the equivalent RB-IGCT withstands the negative voltage. Then, the thyristor recovers the voltage withstanding ability of J_1 and J_3, the thyristor can share the negative voltage. Then, the ac voltage gradually rises from negative voltage to zero crossing to positive voltage. In this process, du/dt is distributed according to the parameter value of the two snubber capacitors parallel to thyristor and IGCT. Therefore, it is necessary to ensure that the snubber capacitance of the equivalent RB-IGCT is smaller than the snubber capacitance of the thyristor, so that the equivalent RB-IGCT firstly withstands the positive voltage and gains a certain amount of time for the thyristor. After the thyristor recovers the voltage withstanding ability of J_2, and then the thyristor withstands more positive voltage. It can be concluded that the IGCT with zero recovery time gives play to the advantage of fast commutation, thus earning more recovery time for the thyristors in the FC-LCC.

From the experiment results shown in Fig. 10(d), we can see that the two IGCTs and four thyristors are formed in series connection to perform 30 kV test. In the experiment, the working procedures of IGCT main switch, thyristor switch, and auxiliary switch are the same as mentioned previously. During the commutation process, the two IGCTs firstly withstand the negative voltage. After the thyristors recovers the voltage withstanding ability, the thyristors and IGCTs share the voltage establishment. The two IGCTs and four thyristors in series connection present the voltage and current distribution.

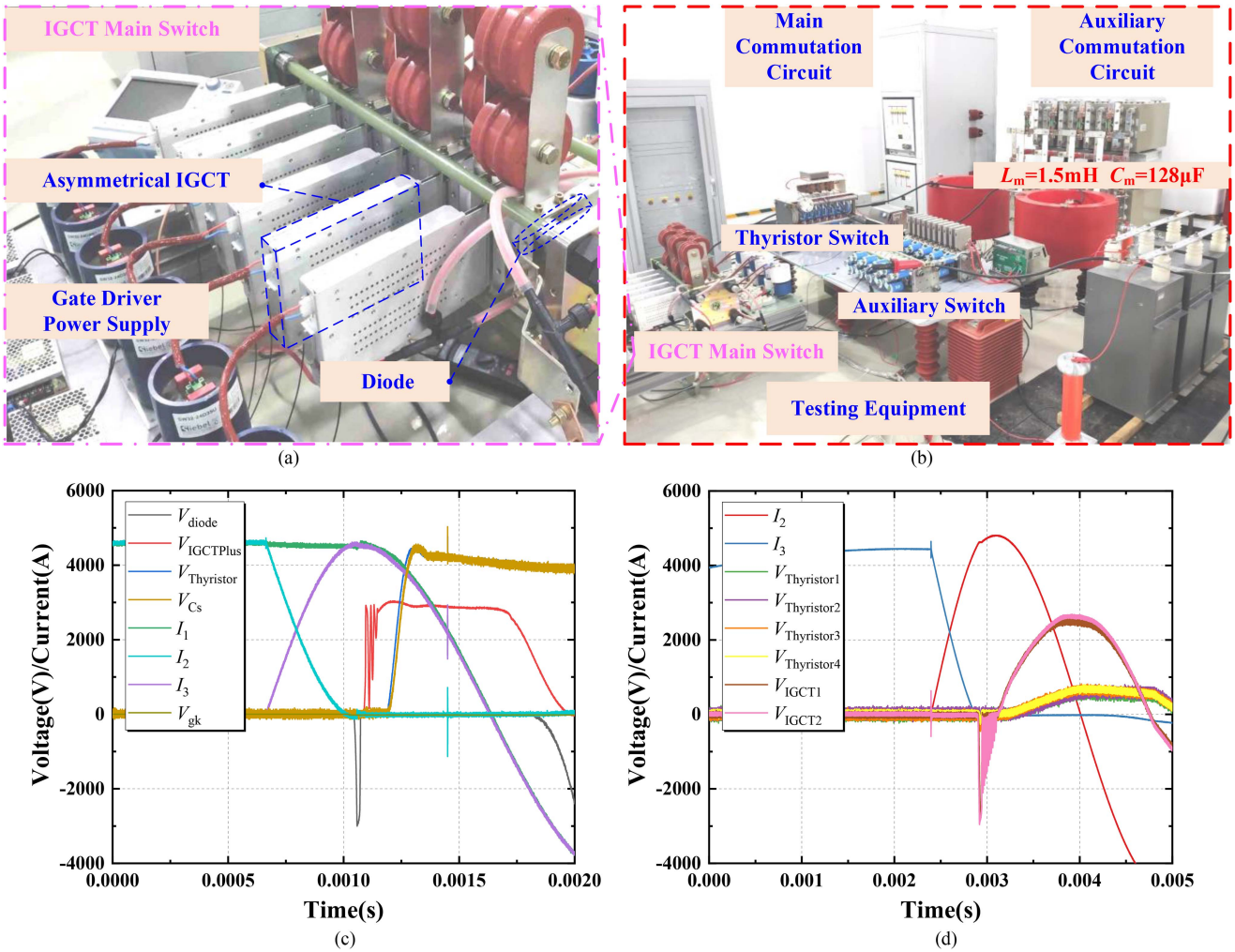

Fig. 10. Comprehensive experiments. (a) Experiment setup of 30 kV/4.5 kA FC-LCC prototype. (b) Experiment platform, including the auxiliary switch, thyristor switch, IGCT switch, auxiliary commutation circuit, and testing equipment. (c) Experimental results of one IGCT and one thyristor in series for 7 kV level test, showing the device characterization of IGCT and thyristor. (d) Experimental results of two IGCTs and four thyristors in series connection for 30 kV level test, showing the voltage and current distribution of IGCTs and thyristors.

As the IGCTs accelerate the voltage establishment in the commutation process, compared with the commutation performance of conventional LCC, the effectiveness and correctness of fast commutation characteristic for the proposed FC-LCC are verified by the experiments.

VII. Conclusion

In this article, the hybrid topology, the control strategy, the hybrid device characterization and interaction, and the design methodology of FC-LCC are deeply and comprehensively analyzed in detail. The FC-LCC creates and utilizes the self-turn-OFF principle of IGCT, giving play to advantage of IGCT's zero commutation time and fast commutation, thus earning more recovery time for the thyristors. The commutation performance of the FC-LCC is enhanced greatly, to mitigate CF.

This article presents the hybrid topology and novel control strategy of self-turn-OFF for fast commutation, and analyzes the hybrid device characterization of thyristor and IGCT. From the theoretical basis, the design methodology of FC-LCC with fast commutation is introduced, and enhances the ability to mitigate CF.

The simulation study based on the CIGRE standard test model in PSCAD/EMTdc is conducted. The fast commutation performance and characteristics are illustrated in the simulation study. The critical grounding inductance is decreased greatly to verify the improvement of CF mitigation capability. A 30 kV/4.5 kA prototype is established and verify the proposed FC-LCC's topology, control strategy, and design methodology. Therefore, the FC-LCC's correctness and effectiveness are verified by the simulation and experiment means. The fast commutation characteristic is trustable.

The proposed scheme can be seen as a promising solution for CF mitigation and has shown significant engineering value for HVdc application.

REFERENCES

[1] C. V. Thio, J. B. Davies, and K. L. Kent, "Commutation failures in HVDC transmission systems," *IEEE Trans. Power Del.*, vol. 11, no. 2, pp. 946–957, Apr. 1996.

[2] Z. Xiaoxin, "Simultaneous commutation failures and forced blocking of multi-in-feed HVDC in east China power grid," in *Proc. CIGRE Large Disturbances Workshop*, 2014, pp. 21–32.

[3] K. Sadek, M. Pereira, D. P. Brandt, A. M. Gole, and A. Daneshpooy, "Capacitor commutated converter circuit configurations for Dc transmission.," *IEEE Trans. Power Del.*, vol. 13, no. 4, pp. 1257–1264, Oct. 1998.

[4] Y. Xue, X.-P. Zhang, and C. Yang, "Elimination of commutation failures of LCC HVDC system with controllable capacitors," *IEEE Trans. Power Syst.*, vol. 31, no. 4, pp. 3289–3299, Jul. 2016.

[5] X. Ni et al., "Enhanced line commutated converter with embedded fully controlled sub-modules to mitigate commutation failures in high voltage direct current systems," *IET Power Electron.*, vol. 9, no. 2, pp. 198–206, 2016.

[6] L. Hou, S. Zhang, Y. Wei, B. Zhao, and Q. Jiang, "A dynamic series voltage compensator for the mitigation of LCC-HVDC commutation failure," *IEEE Trans. Power Del.*, vol. 36, no. 6, pp. 3977–3987, Dec. 2021.

[7] Y. Z. Sun, L. Peng, F. Ma, G. J. Li, and P. F. Lv, "Design a fuzzy controller to minimize the effect of HVDC commutation failure on power system," *IEEE Trans. Power Syst.*, vol. 23, no. 1, pp. 100–107, Feb. 2008.

[8] H.-I. Son and H.-M. Kim, "An algorithm for effective mitigation of commutation failure in high-voltage direct-current systems," *IEEE Trans. Power Del.*, vol. 31, no. 4, pp. 1437–1446, Aug. 2016.

[9] P. Ladoux, N. Serbia, and E. I. Carroll, "On the potential of IGCTs in HVDC," *IEEE J. Emerg. Sel. Topics Power Electron.*, vol. 3, no. 3, pp. 780–793, Sep. 2015.

[10] U. Vemulapati et al., "Recent advancements in IGCT technologies for high power electronics applications," in *Proc. IEEE 17th Eur. Conf. Power Electron. Appl.*, 2015, pp. 1–10.

[11] N. R. Zargari, S. C. Rizzo, Y. Xiao, H. Iwamoto, K. Satoh, and J. F. Donlon, "A new current-source converter using a symmetric gate-commutated thyristor (SGCT)," *IEEE Trans. Ind. Appl.ications*, vol. 37, no. 3, pp. 896–903, May/Jun. 2001.

[12] U. Vemulapati et al., "Reverse blocking IGCT optimised for 1 kV DC bi-directional solid state circuit breaker," *IET Power Electron.*, vol. 8, no. 12, pp. 2308–2314, 2015.

[13] W. Sung, A. Q. Huang, B. J. Baliga, I. Ji, H. Ke, and D. C. Hopkins, "The first demonstration of symmetric blocking SiC gate turn-off (GTO) thyristor," in *Proc. IEEE 27th Int. Symp. Power Semicond. Devices IC's*, 2015, pp. 257–260.

[14] C. Xu et al., "Full-Time junction temperature extraction of IGCT based on Electro-thermal model and TSEP method for high-power applications," *IEEE Trans. Ind. Electron.*, vol. 68, no. 1, pp. 47–58, Jan. 2021.

[15] M. Takei, T. Naito, and K. Ueno, "Reverse blocking IGBT for matrix converter with ultra-thin wafer technology," *IEEE Proc. G Circuits Devices Syst.*, vol. 151, no. 3, pp. 243–247, 2004.

[16] C. Xu et al., "A novel hybrid line commutated converter based on IGCT to mitigate commutation failure for high-power HVdc application," *IEEE Trans. Power Electron.*, vol. 37, no. 5, pp. 4931–4936, May 2022.

[17] X. Zhang et al., "A novel mixture solid-state switch based on IGCT with high capacity and IGBT with high Turn-off ability for hybrid DC breakers," *IEEE Trans. Ind. Electron.*, vol. 67, no. 6, pp. 4485–4495, Jun. 2020.

[18] "IGCT CAc5000-45 plus product datasheet," version 202204, Apr. 2022. [Online]. Available: http://www.sbu.csrzic.com

[19] "HVDC Thyristor KPE5500-85Y04 product datasheet," version 1.0 201603, Mar. 2016. [Online]. Available: http://www.sbu.csrzic.com

Chaoqun Xu was born in Zhejiang, China, in 1996. He received the B.S. degree in 2018 from the Department of Electrical Engineering, Tsinghua University, Beijing, China, where he is currently working toward the Ph.D. degree, both in electrical engineering.

His current research interests include the high power electronic converter, HVdc transmission system, and flexible dc distribution system.

Zhanqing Yu (Member, IEEE) was born in Inner Mongolia, China, in 1981. He received the B.Sc. and Ph.D. degree in electrical engineering from the Department of Electrical Engineering, Tsinghua University, Beijing, China, in 2003 and 2008, respectively.

After graduation, he became a Postdoctor, Lecturer, and an Associate Professor with the Department of Electrical Engineering, Tsinghua University, Beijing, China, in 2008, 2010, and 2012, respectively. He has participated in projects sponsored by High-Tech R&D Program (863 Program), National Basic Research Program of China (973 Program), National Natural Science Foundation of China. His research interests include dc grid, dc breaker, electromagnetic environment, and electromagnetic compatibility.

Biao Zhao (Senior Member, IEEE) was born in Hubei, China, in 1987. He received the B.S. degree from the Department of Electrical Engineering, Dalian University of Technology, Dalian, China, in 2009, and the Ph.D. degree from the Department of Electrical Engineering, Tsinghua University, Beijing, China, in 2014, both in electrical engineering.

He is currently an Associate professor with the Department of Electrical Engineering, Tsinghua University, Beijing, China. His current research interests include high power converter, high power semiconductor device, and flexible dc transmission and distribution system.

Zhengyu Chen was born in Tianjin, China, in 1992. He received the B.S. and Ph.D. degrees in electrical engineering from Tsinghua University, Beijing, China, in 2014 and 2019, respectively.

Then, he became a Joint Postdoctoral Researcher with Tsinghua University and the University of Macau, Macau, China, in 2019. He is currently working at DC Research Center, Energy Internet Research Institute, Tsinghua University. His current research interests include power semiconductor devices and their gate unit drivers, HVdc systems, and dc circuit breakers.

Zongze Wang was born in Henan, China, in 1998. He received the B.S. degree in 2021 from the Department of Electrical Engineering, Tsinghua University, Beijing, China, where he is currently working toward the Ph.D. degree, both in electrical engineering.

His current research interests include the high power electronic converter and HVdc transmission system.

Chunpin Ren was born in Zhejiang, China, in 1997. She received the B.S. degree from the Department of Electrical Engineering, North China Electric Power University, Beijing, China, in 2019. She is currently working toward the Ph.D. degree with the Department of Electrical Engineering, Tsinghua University, Beijing, China, both in electrical engineering.

Her current research interests include high power semiconductor device manufacturing, modeling, and development.

Rong Zeng (Senior Member, IEEE) was born in Shaanxi, China, in 1971. He received the B.Eng., M.Eng., and Ph.D. degrees in electrical engineering from the Department of Electrical Engineering, Tsinghua University, Beijing, China, in 1995, 1997, and 1999, respectively.

He was a Lecturer, Associate Professor, and Professor with the Department of Electrical Engineering, Tsinghua University, in 1999, 2002, and 2007, respectively. He is currently working in the fields of air gap discharge, lightning protection, and electromagnetic compatibility in power systems, electric and magnetic field measurement by integrated electro-optical sensors, power semiconductor, HVdc system, and direct current circuit breaker.